Anomalous Hall effect and magnetic orderings in nanothick V_5S_8

Jingjing Niu and Baoming Yan
State Key Laboratory for Artificial Microstructure and Mesoscopic Physics, Peking University, Beijing 100871, China and Collaborative Innovation Center of Quantum Matter, Beijing 100871, China

Qingqing Ji and Zhongfan Liu
Center for Nanochemistry, Beijing National Laboratory for Molecular Sciences, College of Chemistry and Molecular Engineering, Peking University, Beijing 100871, China

Mingqiang Li
Electron Microscopy Laboratory, School of Physics, Peking University, Beijing 100871, China

Peng Gao
Collaborative Innovation Center of Quantum Matter, Beijing 100871, China and Electron Microscopy Laboratory, School of Physics, Peking University, Beijing 100871, China

Yanfeng Zhang*
Center for Nanochemistry, Beijing National Laboratory for Molecular Sciences, College of Chemistry and Molecular Engineering, Peking University, Beijing 100871, China and Department of Materials Science and Engineering, College of Engineering, Peking University, Beijing 100871, China

Dapeng Yu and Xiaosong Wu†
State Key Laboratory for Artificial Microstructure and Mesoscopic Physics, Peking University, Beijing 100871, China; Collaborative Innovation Center of Quantum Matter, Beijing 100871, China; and Department of Physics, Southern University of Science and Technology of China, Shenzhen 518055, China

(Received 18 February 2017; published 2 August 2017)

The rise of graphene marks the advent of two-dimensional atomic crystals, which have exhibited a cornucopia of intriguing properties, such as the integer and fractional quantum Hall effects, valley Hall effect, charge density waves, and superconductivity, to name a few. Yet, magnetism, a property of extreme importance in both science and technology, remains elusive. There is a paramount need for magnetic two-dimensional crystals. With the availability of many magnetic materials consisting of van der Waals coupled two-dimensional layers, it thus boils down to the question of how the magnetic order will evolve with reducing thickness. Here we investigate the effect of thickness on the magnetic ordering in nanothick V_5S_8. We uncover an anomalous Hall effect, by which the magnetic ordering in V_5S_8 down to 3.2 nm is probed. With decreasing thickness, a breakdown of antiferromagnetism is evident, followed by a spin-glass-like state. For thinnest samples, a weak ferromagnetic ordering emerges. The results not only show an interesting effect of reducing thickness on the magnetic ordering in a potential candidate for magnetic two-dimensional crystals, but demonstrate the anomalous Hall effect as a useful characterization tool for magnetic orderings in two-dimensional systems.

DOI: 10.1103/PhysRevB.96.075402

I. INTRODUCTION

Starting from graphene, the research in two-dimensional (2D) crystals has exploded into a set of subareas covering a vast class of materials, including hexagonal boron nitride, transition metal dichalcogenides, silicene and phosphorene, etc. [1–3]. With a broad spectrum of properties displayed by 2D crystals on hand, it is tempting to construct van der Waals heterostructures by multistacking so that the material functionality can be greatly expanded [1]. However, magnetism, a property that has been playing an indispensable role in both science and technology, remains elusive in 2D crystals. On one hand, since most 2D crystals are nonmagnetic, studies have mainly been focused on induced magnetism by defects and adatoms [4–10]. On the other hand, it has been actively pursued to find 2D crystals that are intrinsically magnetic [11–14]. The natural approach is to start with known three-dimensional (3D) magnetic materials that consist of weakly bonded 2D layers and investigate how the thickness affects the magnetic ordering. In addition, revealing the evolution can deepen our understanding on phase transitions in low-dimensional systems.

However, the experiment is challenging when one tries to characterize the magnetic properties of 2D crystals. This is because common tools for magnetization characterization, such as magnetometers, neutron scattering, and the magnetic resonance technique, often require a 3D bulk sample. To study the magnetic property of a single 2D crystal, new and simple methods are highly desired. Raman spectroscopy, combined with theoretical calculations, was employed to infer

*yanfengzhang@pku.edu.cn
†xswu@pku.edu.cn

the antiferromagnetic ordering in atomic layers of $FePS_3$ [13,14]. Recent studies have utilized the Kerr effect to identify ferromagnetic ordering in 2D materials in the monolayer limit [15,16].

In this work, we study the thickness dependence of the magnetic ordering in V_5S_8 nanoflakes. An unusual Hall behavior is found. It is convincingly shown that it stems from the anomalous Hall effect (AHE). The effect enables characterization of the magnetic ordering of a single nanoflake. The thickness dependence of the AHE, combined with magnetoresistance (MR), reveals a breakdown of antiferromagnetism (AFM) with reducing thickness. For thinnest flakes, a weak ferromagnetism (FM) emerges. In the transition region, the competition between AFM and FM interactions gives rise to a spin-glass-like state. Our results not only reveal an interesting effect of reducing thickness on the magnetic ordering in a potential candidate of a magnetic 2D crystal, but also demonstrate the anomalous Hall effect as a useful tool for obtaining information on the magnetic ordering in 2D crystals.

II. EXPERIMENTAL TECHNIQUES

V_5S_8 flakes were grown at 600 °C by a chemical vapor deposition method using solid VCl_3 and sulfur precursors under a mixed Ar/H_2 gas flow. By lowering the evaporation temperature of VCl_3 down to 275–300°C and optimizing the location of SiO_2/Si substrates at 6 cm downstream from the VCl_3 precursor, V_5S_8 nanoflakes with thickness less than 10 nm and domain size up to tens of micrometers could be readily synthesized. The V_5S_8 samples could be further thinned down to 3.2 nm (2.5 unit cell) by peeling off the as-grown nanoflakes onto fresh SiO_2/Si substrates.

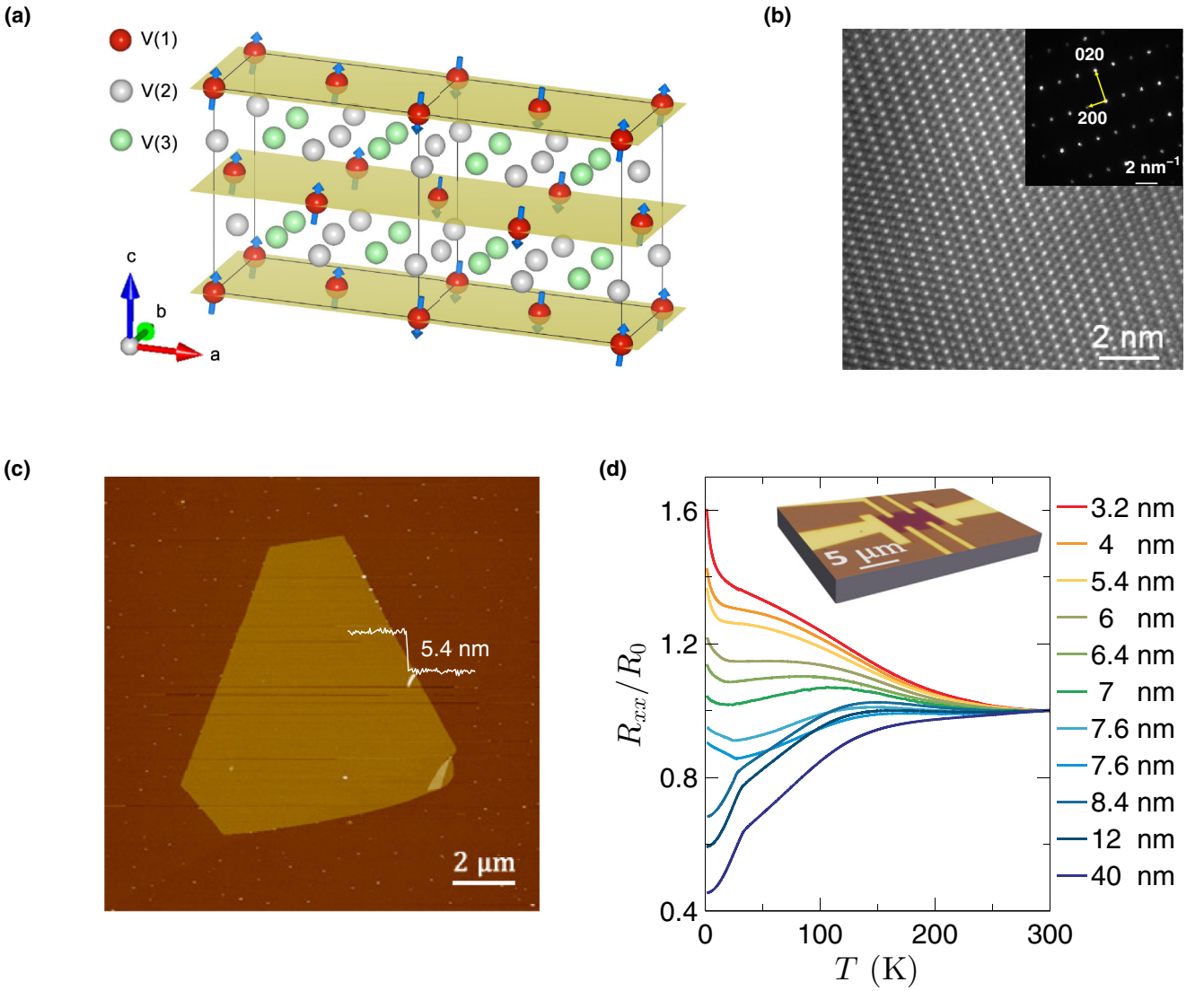

FIG. 1. Structure, morphology, and resistivity of V_5S_8 flakes. (a) Unit cell of the magnetic structure of V_5S_8, whose volume is doubled compared with the crystalline unit cell (a is doubled). (b) High-resolution TEM image of a nanosheet with viewing direction of [001]. Inset is the corresponding selected area electron diffraction pattern. (c) Atomic force microscopy image of a 5.4-nm-thick flake. The white line shows the height profile across an edge of the flake. (d) Temperature dependence of the resistivity normalized to the resistivity at 300 K, $R/R_{300\,\mathrm{K}}$, for samples of different thickness. For clarity, only a part of the samples are shown. More data can be found in the Supplemental Material. Inset: A typical Hall bar structure used in the measurements.

Consequently, two types of thin samples were measured: as-grown and thinned by mechanical exfoliation of thicker flakes. No significant difference was found (see Figs. S2 and S3 in the Supplemental Material [17]). Samples are very stable in ambient conditions, as the optical contrast and the resistance stayed the same after days of exposure even in the thinnest samples. Bulk samples of V_5S_8 were purchased from The 2D AGE Company. High-resolution transmission electron microscopy imaging and electron diffraction experiments was performed in an FEI Tecnai F30 TEM at 300 kV. The atomic force microscopy image was captured on a Bruker Dimension Icon AFM. Standard electron beam lithography was employed to pattern the Hall bar structure and 5 nm Pd/80 nm Au was used for metallization. As samples are metallic and stable, no special care is needed to ensure a good electrical contact ($<100\ \Omega$). Four-probe electrical measurements were carried out using a lock-in method in an Oxford variable temperature cryostat. All magnetotransport measurements were performed with the magnetic field perpendicular to the film plane. Magnetization measurements were performed in a Magnetic Property Measurement System by Quantum Design.

III. RESULTS AND DISCUSSIONS

A. Crystal and magnetic structures of V_5S_8

V_5S_8 is a layered material and can be viewed as VS_2 intercalated with V atoms. It has a monoclinic structure ($a = 11.396$ Å, $b = 6.645$ Å, $c = 11.293$ Å, $\alpha = \gamma = 90°$, $\beta = 91.45°$), space group $F2/m$, shown in Fig. 1(a) [18]. The VS_2 layer is in a distorted $1T$ structure due to V intercalation. The intercalated V atoms are below V atoms in the VS_2 layer. Therefore, there are three inequivalent V sites: V(1), V(2), and V(3). Intercalated V atoms are on the V(1) sites, forming a slightly distorted triangular lattice. The magnetic properties of bulk V_5S_8 are more or less understood [19–25]. It is an antiferromagnetic metal below about 32 K. Neutron scattering and nuclear magnetic resonance experiments have suggested that the intercalated V atoms are responsible for the magnetism. Their spins align at 10.4° away from the c axis toward the a axis. The antiferromagnetic alignment of spins is depicted in Fig. 1. The resistivity is metallic and displays a kink at 32 K, which has been identified as the Néel temperature T_N (see the Supplemental Material). When a magnetic field is applied parallel to the c axis, a spin-flop (SF) transition occurs at a critical field $H_c \approx 3.5$ T [21,25]. The AFM ordering persists down to 10 nm [26].

We have studied thin flakes of V_5S_8 samples with a series of thickness down to 3.2 nm. Monolayer V_5S_8, consisting of two layers of VS_2 and one layer of intercalated V, is 0.847 nm thick and each subsequent layer adds an additional 0.565 nm to the thickness. So, 3.2 nm roughly corresponds to five layers. It is worth noting that the interface between the substrate and the 2D material may additionally contribute to the thickness, too. The structure is confirmed by the transmission electron microscopy (TEM) characterization in Fig. 1 and Supplemental Material Fig. S1. A high-resolution image in Fig. 1(b) shows the structure of a nanoflake V_5S_8 and the selected area electron diffraction pattern exhibits a rectangular arrangement with $d_{200} = 5.75 \pm 0.05$ Å and $d_{020} = 3.35 \pm 0.05$ Å, from which the lattice constants are calculated to be about $a = 1.15$ nm and $b = 0.67$ nm, in agreement with V_5S_8 [20,27]. However, sometimes we did observe rotation of the a and b axes and the hexagonal lattice of VS_2, suggesting the existence of intercalation fluctuations. For thicker flakes, the resistance decreases with temperature and is followed by a sudden drop at 32 K, signaling an AFM transition. The dependence is similar to bulk materials (see the Supplemental Material). Interestingly, when the thickness is below 8.4 nm or so, the resistance drop at 32 K becomes an abrupt increase, maintaining a well-defined transition temperature. With further reduction of the thickness, the sharp transition turns into a crossover. Although the low-temperature enhancement of the resistivity is stronger in thinner flakes, it remains relatively low down to 3.2 nm, suggesting an absence of strong localization or opening up of a gap.

B. Magnetotransport and anomalous Hall effect in thick flakes

In thicker flakes, the SF transition in the AFM state is clearly manifested in magnetotransport. Figure 2 shows the MR and

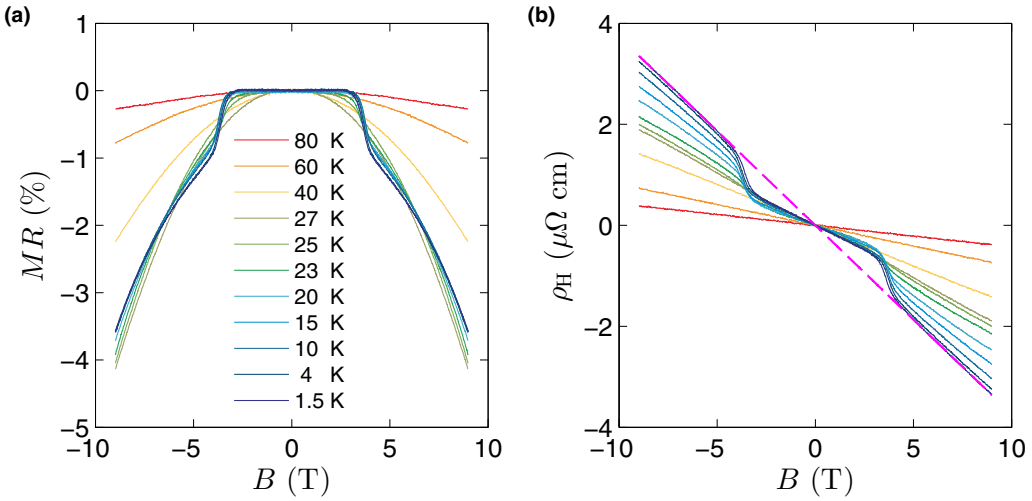

FIG. 2. Magnetotransport of an 8.4-nm-thick flake. (a) MR at different temperatures. (b) ρ_H at different temperatures. The magenta dashed line is a linear fit of the high-field data.

Hall resistivity ρ_H for a typical sample (data for more samples can be found in the Supplemental Material). Below T_N, the low-field resistance is essentially constant, followed by a sudden decrease at 3.5 T, which results from the SF transition. No appreciable hysteresis has been observed, probably due to a flat barrier between two states on two sides of the transition [28]. The high-field dependence is quadratic and diminishes with temperature, consistent with suppression of scattering from local spin fluctuations in a paramagnetic (PM) state [29,30]. The SF transition indicates a relatively weak spin anisotropy [31,32]. In fact, the anisotropy in bulk V_5S_8 was found to be extremely small [22].

Accordingly, ρ_H exhibits an intriguing change of the slope across the SF transition, seen in Fig. 2(b). A nonlinear Hall resistivity usually indicates a two-band conduction, but the fact that the high-field Hall extrapolates exactly to the origin rules out this possibility, as a simple two-band model cannot reproduce such a behavior. Another explanation would be a field-induced change of the carrier density; for instance, breaking down of a spin-density wave state. But, a spin-density wave gaps out a part of the Fermi surface. Thus, its breaking down would recover the gapped Fermi surface, hence increasing the carrier density. The resultant reduction of the Hall resistance is apparently at odds with the experiment, not to mention that no spin-density wave has been reported in the material before.

In magnetic materials, the Hall resistivity consists of two contributions, $\rho_H = R_0 B + R_{AHE}\mu_0 M$, where R_0 and R_{AHE} are the ordinary and anomalous Hall coefficients, M is the magnetization, and μ_0 the vacuum permeability. Although the AHE often appears in an FM metal, it can also occur in a PM or AFM one [33–36]. The difference is that the AHE is linear in B for the latter, as M is also linear in B. In our samples, a magnetic field induces a SF transition, which results in an increase of the magnetic susceptibility, hence ρ_H.

To verify this hypothesis, we need to measure M, which can be directly measured only for bulk materials. So, the magnetization and transport measurements were carried out for a bulk V_5S_8 (see Fig. S4 in the Supplemental Material). A linear relation between $\mu_0 M/B$ and ρ_H/B was indeed found, confirming the contribution of the AHE (see Fig. S5 and the discussion in the Supplemental material). Moreover, R_{AHE} has a sign opposite to R_0. $R_0 = 0.20\ \mu\Omega$ cm T^{-1}, corresponding to a hole density of 3.13×10^{21} cm^{-3}. The carrier being hole is corroborated by the positive slope of the gate dependence of resistivity for a very thin sample, seen in Supplemental Material Fig. S9. Apparently, ρ_H is dominated by negative R_{AHE}. Therefore, the linear dependence between R_{AHE} and $\mu_0 M/B$ provides us with a desperately needed means to

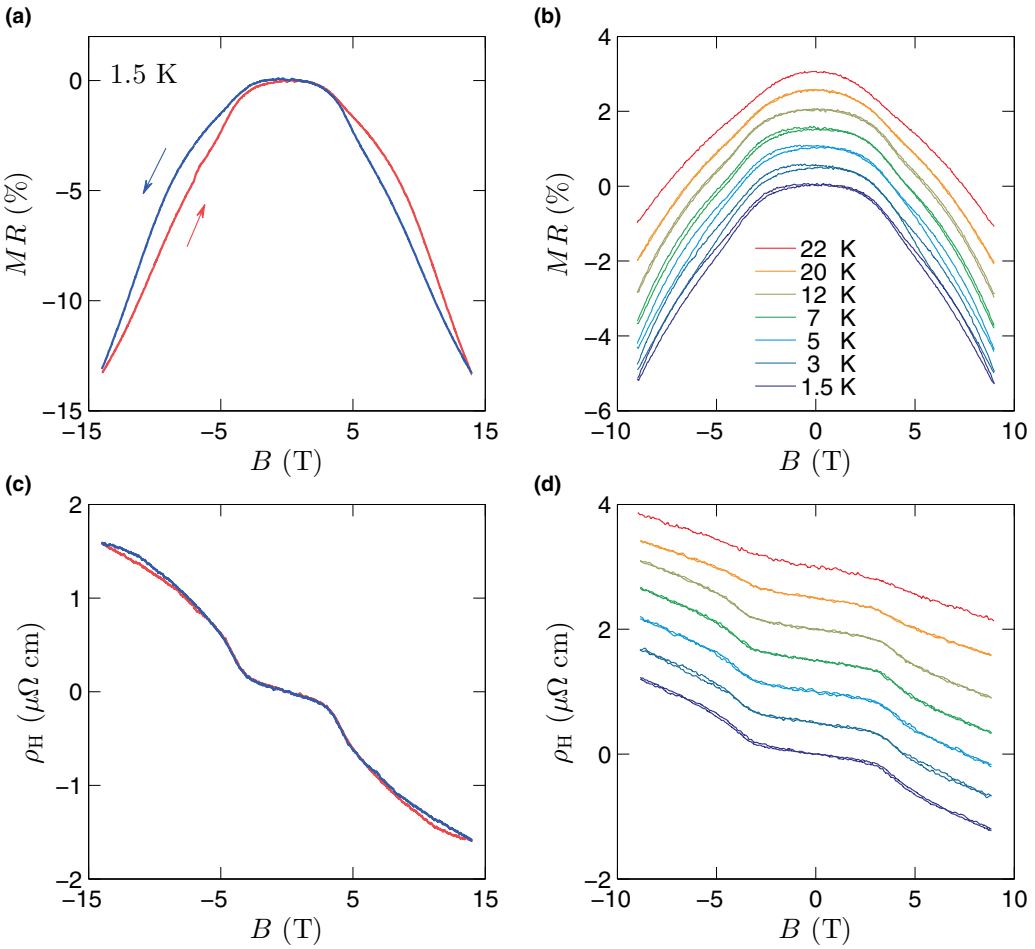

FIG. 3. Magnetotransport of a 7.6-nm-thick flake. (a) MR hysteresis at 1.5 K. (b) MR at different temperatures. (c) ρ_H hysteresis at 1.5 K. (d) ρ_H at different temperatures.

gain the information on the magnetization of individual 2D crystals, which is inaccessible, due to their negligible volume, to magnetometers and magnetic resonance techniques. R_{AHE} for the bulk is $-162.41\ \mu\Omega\,\mathrm{cm\,T^{-1}}$, calculated from the slope in Fig. S5. The longitudinal resistivity ρ_{xx} is around 600 $\mu\Omega$ cm. In this regime, we evaluate the magnitude of the AHE by calculating $S = \mu_0 R_{\mathrm{AHE}}/\rho_{xx}^2 = -0.057\ \mathrm{V^{-1}}$. It is of the same order as in various magnets [34,37]. Being dominated by the AHE, in what follows, the Hall can be simply viewed as the magnetization.

As the thickness is reduced below 8.4 nm, the low-temperature resistivity goes up. The SF transition is not as sharp as in thicker flakes. In addition, the magnetotransport becomes hysteretic, suggesting a spin-glass-like state. Typical data for a 7.6-nm-thick flake are shown in Fig. 3. The hysteresis is only significant above H_c. Its magnitude increases with the sweeping field and decreases with temperature and eventually disappears at about 12 K. The nonlinear ρ_{H}, on the other hand, persists to a higher temperature. The hysteresis in MR is more pronounced than that in ρ_{H}. Since the in-plane magnetization does not contribute to the AHE, but to MR via spin fluctuation scattering, it is speculated that the hysteresis is mainly related to the in-plane spin component.

C. Anomalous Hall effect and ferromagnetic ordering in thin flakes

With further reduction of thickness, the nonlinearity of ρ_{H} diminishes. H_c becomes smaller and the low-field slope approaches the high-field one. However, when the thickness is below about 5.4 nm, the Hall behavior qualitatively changes. A steep slope emerges in low fields, while it remains linear in high fields, shown in Fig. 4. The high-field linear dependence intercepts the y axis at a finite value, in sharp contrast with the zero intercept in thick flakes. After subtracting a high-field linear background, the nonlinear part $\rho_{\mathrm{H}}^{\mathrm{nl}}$ is extracted and plotted in Fig. 4(b). The curves exhibit characteristics of the AHE of an FM metal, suggesting an FM ordering. The saturation value of $\rho_{\mathrm{H}}^{\mathrm{nl}}$, which is proportional to the saturation magnetization, decreases with temperature. Its temperature dependence is plotted in the inset of Fig. 4(b), from which the Curie temperature can be estimated to be 7 K.

A similar FM type of the AHE has been observed in other thin flakes as well, seen in Figs. 4(c) and 4(d). No hysteresis has been observed, indicating a rather soft FM, consonant with the weak spin anisotropy indicated by the SF transition as we discussed above. The amplitude of the AHE ranges from 0.01 to 0.1 $\mu\Omega$ cm. The fact that the linear

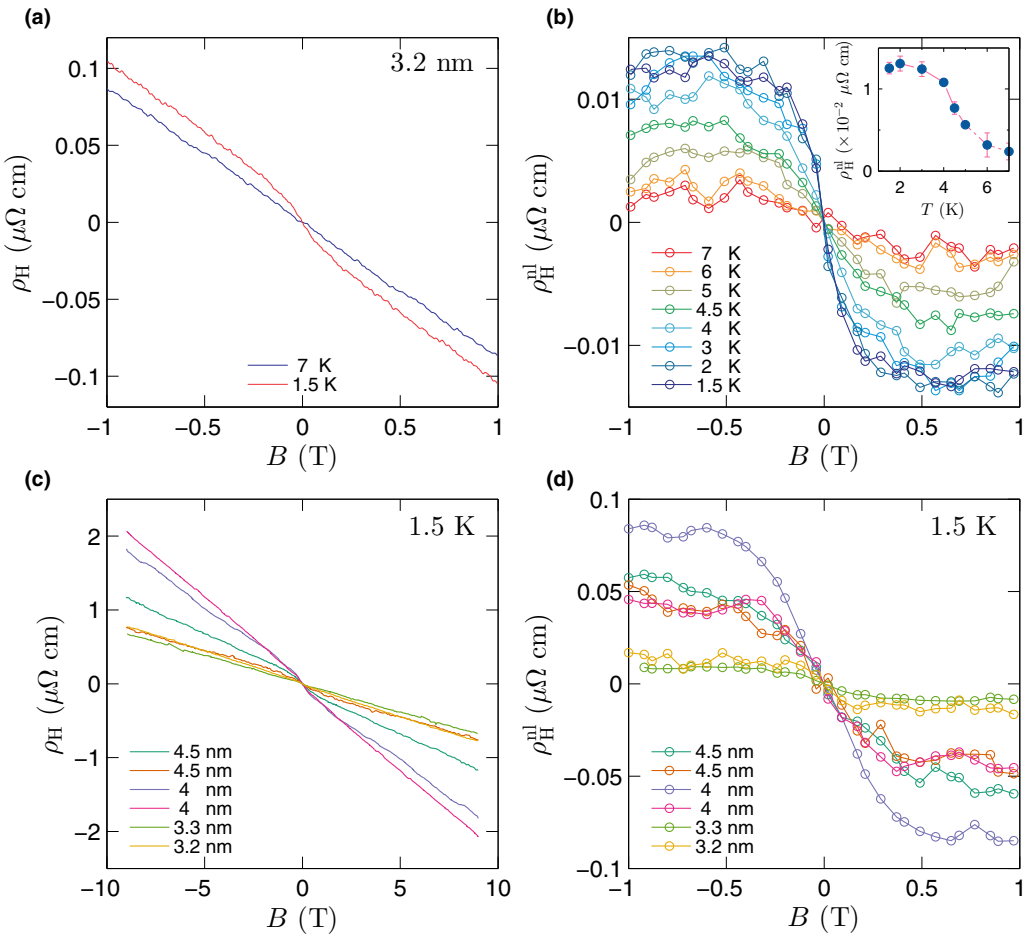

FIG. 4. ρ_{H} of a 3.2-nm-thick flake. (a) ρ_{H} at 1.5 (red) and 7 (blue) K. (b) Nonlinear Hall resistivity $\rho_{\mathrm{H}}^{\mathrm{nl}}$ obtained by subtracting the high-field linear background at different temperatures. Inset: Saturation value (averaged over the higher-field region) of $\rho_{\mathrm{H}}^{\mathrm{nl}}$ as a function of temperature. (c) ρ_{H} of other measured thin flakes at 1.5 K. (d) Nonlinear Hall resistivity $\rho_{\mathrm{H}}^{\mathrm{nl}}$.

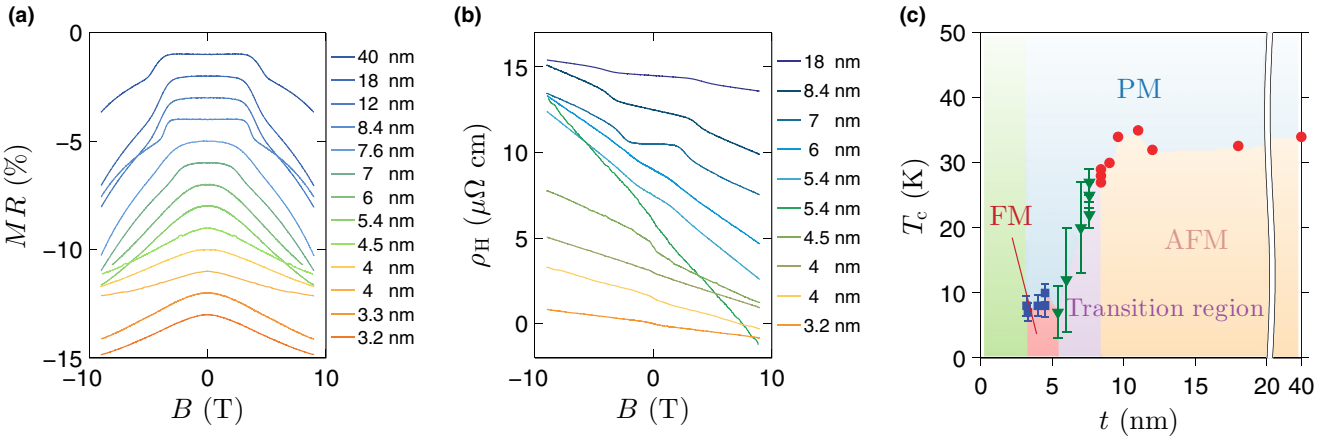

FIG. 5. Thickness dependence of magnetotransport and the phase diagram. Evolution of (a) MR and (b) ρ_H with thickness at 1.5 K. For clarity, only a part of the samples are shown. More data can be found in the Supplemental Material. (c) Critical temperature T_c–thickness t phase diagram.

AHE is large and nonsaturating implies that only a fraction of the magnetic moments participate in the FM ordering, while the rest remain in a PM state. This may be due to residual competition between FM and AFM interactions and inhomogeneity of intercalation. Alternatively, it could be related to the enhanced thermal fluctuation effect in reduced dimensions, which suppresses a long-range order in a Heisenberg spin system, as observed in $Cr_2Ge_2Te_6$ [15]. Although V_5S_8 bulk is an Ising antiferromagnet, the weak spin anisotropy may push thin layers toward a weakly anisotropic Heisenberg spin system. Further study on thinner flakes and with improved sample growth techniques is needed to unveil the origin.

D. Magnetic phase diagram

To give an overall picture of the evolution of transport properties with thickness, the low-temperature MR and Hall resistivity for samples of a series of thicknesses are plotted in Figs. 5(a) and 5(b). For thicker samples, MR shows a plateau in low fields and a sudden drop at the critical field H_c of the SF transition, followed by a quadratic field dependence. Correspondingly, the Hall displays a jump at H_c. As the thickness goes below 8.4 nm, the SF transition fades out. In particular, the discontinuity in MR and Hall is smeared out and H_c is reduced. At last, the MR is quadratic except for a tendency toward a sublinear dependence in high fields. The Hall is close to linear, suggesting a dominant PM behavior. With further decreasing thickness, an FM order develops, evidenced by a nonlinear AHE. From these observations, we are able to plot the magnetic phase diagram of the material as a function of thickness, illustrated in Fig. 5(c).

An intriguing thickness-induced magnetic phase transition is observed in V_5S_8. In contrast, the AFM ordering in $FePS_3$ has been found to persist down to monolayer [13,14]. The phase transition we observed stems from competing AFM and FM interactions, which are manifested in the spin-glass-like state between the AFM and FM phases. The existence of an FM interaction is not surprising, as it can be inferred from the AFM ordering in the bulk material, shown in Fig. 1(c). Along the x direction, the magnetic moments align in an alternating fashion, parallel and antiparallel. The parallel alignment suggests an FM interaction, which is in fact implied by a positive Currie-Weiss temperature, reported in previous studies [19,22] and observed in the current work (see the Supplemental Material), as well. Thus, the reduction of thickness changes the balance between FM and AFM interactions, leading to the emergence of an FM ordering. Various mechanisms can potentially contribute to the dependence of the magnetic interactions on thickness, e.g., modification of the energy band due to quantum confinement, or change of the interlayer coupling. More work is required to identify and understand the effect.

IV. CONCLUSION

Our findings demonstrate the AHE as a useful tool for magnetization characterization of 2D crystals and reveal an intriguing magnetic phase transition induced by reduced dimensionality in V_5S_8. Besides potential applications in spintronics, such materials could provide a new playground for studying magnetism, as not only the low dimensionality can qualitatively change the phenomenon, but the tunability of 2D materials enables studies over parameter spaces that are difficult or even impossible to access. In our thinnest samples, we have been able to see an appearance of the gate tunability. Furthermore, compared with these newly found magnetic 2D materials, such as CrI_3, $FePS_3$, and $Cr_2Ge_2Te_6$ [13–16], V_5S_8 is unique in that it is very stable in air and conductive. It may be an ideal platform for studying itinerant-electron magnetism in 2D.

ACKNOWLEDGMENTS

This work was supported by The National Key Research and Development Program of China (Grants No. 2016YFA0300600, No. 2013CBA01603, and No. 2016YFA0300802) and NSFC (Projects No. 11574005, No. 11222436, No. 11234001, No. 51290272, and No. 51472008).

J.N. and Q.J. contributed equally to this work.

[1] A. K. Geim and I. V. Grigorieva, Nature (London) **499**, 419 (2013).

[2] S. Z. Butler, S. M. Hollen, L. Cao, Y. Cui, J. A. Gupta, H. R. Gutiéez, T. F. Heinz, S. S. Hong, J. Huang, A. F. Ismach, E. Johnston-Halperin, M. Kuno, V. V. Plashnitsa, R. D. Robinson, R. S. Ruoff, S. Salahuddin, J. Shan, L. Shi, M. G. Spencer, M. Terrones, W. Windl, and J. E. Goldberger, ACS Nano **7**, 2898 (2013).

[3] L. Li, Y. Yu, G. J. Ye, Q. Ge, X. Ou, H. Wu, D. Feng, X. H. Chen, and Y. Zhang, Nat. Nanotechnol. **9**, 372 (2014).

[4] J. Zhang, J. M. Soon, K. P. Loh, J. H. Yin, J. Ding, M. B. Sullivian, and P. Wu, Nano Lett. **7**, 2370 (2007).

[5] Y. Wang, Y. Huang, Y. Song, X. Zhang, Y. Ma, J. Liang, and Y. Chen, Nano Lett. **9**, 220 (2009).

[6] S. Tongay, S. S. Varnoosfaderani, B. R. Appleton, J. Wu, and A. F. Hebard, Appl. Phys. Lett. **101**, 123105 (2012).

[7] R. R. Nair, M. Sepioni, I.-L. Tsai, O. Lehtinen, J. Keinonen, A. V. Krasheninnikov, T. Thomson, A. K. Geim, and I. V. Grigorieva, Nat. Phys. **8**, 199 (2012).

[8] R. R. Nair, I.-L. Tsai, M. Sepioni, O. Lehtinen, J. Keinonen, A. V. Krasheninnikov, A. H. C. Neto, M. I. Katsnelson, A. K. Geim, and I. V. Grigorieva, Nat. Commun. **4**, 2010 (2013).

[9] W. Han, R. K. Kawakami, M. Gmitra, and J. Fabian, Nat. Nanotechnol. **9**, 794 (2014).

[10] H. González-Herrero, J. M. Gómez-Rodrguez, P. Mallet, M. Moaied, J. J. Palacios, C. Salgado, M. M. Ugeda, J.-Y. Veuillen, F. Yndurain, and I. Brihuega, Science **352**, 437 (2016).

[11] K.-z. Du, X.-z. Wang, Y. Liu, P. Hu, M. I. B. Utama, C. K. Gan, Q. Xiong, and C. Kloc, ACS Nano **10**, 1738 (2016).

[12] J.-G. Park, J. Phys.: Condens. Matter **28**, 301001 (2016).

[13] J.-U. Lee, S. Lee, J. H. Ryoo, S. Kang, T. Y. Kim, P. Kim, C.-H. Park, J.-G. Park, and H. Cheong, Nano Lett. **16**, 7433 (2016).

[14] X. Wang, K. Du, Y. Y. F. Liu, P. Hu, J. Zhang, Q. Zhang, M. H. S. Owen, X. Lu, C. K. Gan, P. Sengupta, C. Kloc, and Q. Xiong, 2D Mater. **3**, 031009 (2016).

[15] C. Gong, L. Li, Z. Li, H. Ji, A. Stern, Y. Xia, T. Cao, W. Bao, C. Wang, Y. Wang, Z. Q. Qiu, R. J. Cava, S. G. Louie, J. Xia, and X. Zhang, Nature **546**, 265 (2017).

[16] B. Huang, G. Clark, E. Navarro-Moratalla, D. R. Klein, R. Cheng, K. L. Seyler, D. Zhong, E. Schmidgall, M. A. McGuire, D. H. Cobden, W. Yao, D. Xiao, P. Jarillo-Herrero, and X. Xu, Nature **546**, 270 (2017).

[17] See Supplemental Material at http://link.aps.org/supplemental/10.1103/PhysRevB.96.075402 for more transport and magnetization measurements.

[18] I. Kawada, M. Nakano-Onoda, M. Ishii, M. Saeki, and M. Nakahira, J. Solid State Chem. **15**, 246 (1975).

[19] A. D. Vries and C. Haas, J. Phys. Chem. Solids **34**, 651 (1973).

[20] B. G. Silbernagel, R. B. Levy, and F. R. Gamble, Phys. Rev. B **11**, 4563 (1975).

[21] H. Nozaki and Y. Ishizawa, Phys. Lett. A **63**, 131 (1977).

[22] H. Nozaki, M. Umehara, Y. Ishizawa, M. Saeki, T. Mizoguchi, and M. Nakahira, J. Phys. Chem. Solids **39**, 851 (1978).

[23] Y. Kitaoka and H. Yasuoka, J. Phys. Soc. Jpn. **48**, 1949 (1980).

[24] S. Funahashi, H. Nozaki, and I. Kawada, J. Phys. Chem. Solids **42**, 1009 (1981).

[25] M. Nakanishi, K. Yoshimura, K. Kosuge, T. Goto, T. Fujii, and J. Takada, J. Magn. Magn. Mater. **221**, 301 (2000).

[26] W. J. Hardy, J. Yuan, H. Guo, P. Zhou, J. Lou, and D. Natelson, ACS Nano **10**, 5941 (2016).

[27] P. Poddar and A. K. Rastogi, J. Phys.: Condens. Matter **14**, 2677 (2002).

[28] Y. S. Oh, S. Artyukhin, J. J. Yang, V. Zapf, J. W. Kim, D. Vanderbilt, and S.-W. Cheong, Nat. Commun. **5**, 3201 (2014).

[29] H. Yamada and S. Takada, Prog. Theor. Phys. **48**, 1828 (1972).

[30] K. Jin, G. He, X. Zhang, S. Maruyama, S. Yasui, R. Suchoski, J. Shin, Y. Jiang, H. S. Yu, J. Yuan, L. Shan, F. V. Kusmartsev, R. L. Greene, and I. Takeuchi, Nat. Commun. **6**, 8183 (2015).

[31] H. D. Groot and L. D. Jongh, Physica B&C (Amsterdam) **141**, 1 (1986).

[32] K. Balamurugan, S.-H. Lee, J.-S. Kim, J.-M. Ok, Y.-J. Jo, Y.-M. Song, S.-A. Kim, E. S. Choi, M. D. Le, and J.-G. Park, Phys. Rev. B **90**, 104412 (2014).

[33] A. Fert and O. Jaoul, Phys. Rev. Lett. **28**, 303 (1972).

[34] S. Nakatsuji, N. Kiyohara, and T. Higo, Nature (London) **527**, 212 (2015).

[35] Y. Luo, F. Ronning, N. Wakeham, X. Lu, T. Park, Z.-A. Xu, and J. D. Thompson, Proc. Natl. Acad. Sci. U.S.A. **112**, 13520 (2015).

[36] T. Suzuki, R. Chisnell, A. Devarakonda, Y.-T. Liu, W. Feng, D. Xiao, J. W. Lynn, and J. G. Checkelsky, Nat. Phys. **12**, 1119 (2016).

[37] N. Nagaosa, J. Sinova, S. Onoda, A. H. MacDonald, and N. P. Ong, Rev. Mod. Phys. **82**, 1539 (2010).